A NOVEL CONCEPT FOR A POSITRON EMISSION TOMOGRAPHY SCANNER

An Undergraduate Research Scholars Thesis

by

BRIAN KELLY, MATTHEW LEE

ELLIOT LEVIN and JEENA KHATRI

Submitted to Honors and Undergraduate Research
Texas A&M University
in partial fulfillment of the requirements for the designation as an

UNDERGRADUATE RESEARCH SCHOLAR

Approved by
Research Advisor: Dr. Rupak Mahapatra

May 2015

Major: Physics

TABLE OF CONTENTS

ABSTRACT

A Novel Concept for a Positron Emission Tomography Scanner. (May 2015)

Brian Kelly, Matthew Lee, Elliot Levin and Jeena Khatri
Department of Physics
Texas A&M University

Research Advisor: Dr. Rupak Mahapatra
Department of Physics

Positron Emission Tomography (PET) allows physicians and researchers to visualize metabolic data in the human body and is widely used in cancer and neurological imaging. Traditional PET scanners consist of a thin ring of scintillators coupled to photo detectors but these scanners often take long periods of time to acquire an image, are very costly, and are too complex to fit inside other machinery such as MRI. In response to this, we are building a novel PET detector that utilizes non-traditional scintillators and photo detectors in an attempt to significantly decrease cost, allow combined PET/MRI modalities and reduce scan time.

CHAPTER I

INTRODUCTION

As medicine has advanced alongside technology in the twentieth and twenty-first century, there has been a shift from treatments based solely on exterior signs and symptoms to treatments based on a combination of both interior and exterior signs and symptoms. As one would imagine, the ability to understand what is happening inside the body, without harming a patient, has provided doctors with tremendously better opportunities to properly treat and monitor patients. Before Rontgen's discovery of x-rays in the late nineteenth century, the only way to understand what was happening inside of a patient was through surgery, which, obviously, often did more damage than good. When it was discovered that, using x-rays, physicians could obtain images of internal structures in the body – namely bones – a whole new branch of science at the interface of medicine, physics and engineering quickly began to develop: medical imaging.

While the first medical images were very crude and involved high levels of radiation, scientists, engineers and physicians were able to advance the field to a much safer, practical level. Around 1970, the first commercial x-ray computed tomography (CT) scanner – a machine that allowed physicians to obtain three-dimensional images of interior tissue – was released. This modality is still used today to obtain high resolution, three-dimensional images of the human body. Combined with Magnetic Resonance Imaging (MRI) – another modality that obtains high-resolution structural images – physicians are now able to see the inside of the human body in unprecedented detail.

As advances were made in structural imaging, physicians began to see a need to understand not only what the inside of the body looks like, but also to understand underlying physiological processes – things such as cellular metabolism and neural signal transmission. This area of imaging, called functional imaging, would ideally be combined with structural imaging, so that physicians may understand precisely what is happening at what locations in the body. A variety of approaches including lasers, functional MRI (fMRI) and nuclear science methods are currently used to obtain functional images. This thesis, however, will focus on one particular modality of functional imaging – Positron Emission Tomography (PET).

Positron emission tomography for functional imaging

Positron Emission Tomography (PET) is a functional imaging technique that holds several advantages over related methods. To start, it is very diverse. PET may be used to obtain functional images of things such as cancerous tissue (probably the most common application), neural activity and even intestinal disease and malfunction (Ollinger 1997). Furthermore, PET outperforms other similar approaches such as gamma cameras or single-photon emission computed tomography (SPECT) by having lower cost, better image formation (higher signal-to-noise ratio) and by being cheaper overall.

A PET scan begins with the intake of a radiopharmaceutical (a radioactive isotope attached to a common biological molecule) by the patient. After a short delay, this radiopharmaceutical will begin to concentrate in the targeted areas. In the example of cancer imaging, a patient ingests a glucose-based radiopharmaceutical that will concentrate in areas of high cellular metabolism, indicating that cancer is likely present. Within the patient's body, the radiopharmaceutical will begin to decay and release positrons, which travel a short distance (on the order of 1 centimeter) in the patient before annihilating with an electron. The annihilation will result in the release of two back-to-back photons, each with energy 511 keV that will be collected by a ring of detectors surrounding the patient. The signals collected from the release of these photons may then be digitized and sent to a computer for processing into a functional image. This image is then often combined with a high-quality structural image – MRI or CT – so that physicians may understand the physiological processes happening at different areas within the body.

Current PET technology

Modern PET scanners, while bulky and very expensive, provide decent image qualities on a centimeter-level resolution. While nowhere near the quality of MRI or CT scanners (which now have the ability to resolve individual blood vessels), these images provide the necessary functional information that physicians need.

The two most critical parts of a PET scanner are scintillators and photodetectors. Scintillators are special crystals that release light upon excitation by an external stimulus, be it vibrations, charged particles or photons. In PET, a scintillator will be excited by the 511 keV photons and release light in the ultraviolet range. This ultraviolet light is then collected by a photodetector that turns the optical signal into an electrical signal. In modern scanners, the most commonly used scintillators are inorganic – LSO, LYSO, BGO, etc. While these scintillators are very efficient at photon detection and have very short decay rates (allowing time discrimination and higher resolution), they are also very expensive. The most commonly used photodetectors in modern scanners are photomultiplier tubes. These tubes, to be fully explained later, are also very efficient and fast, but, much like inorganic scintillators, are very expensive. Recent literature has begun to question the viability of using these components when it may be possible to achieve comparable, or even better, results, using cheaper material.

Basic Image Formation

As previously mentioned, during a PET scan, data collection is achieved by a ring of detectors surrounding the patient. When an annihilation event occurs, antiparallel photons will be released from the patient and collected by two scintillator-photodetector pairs (hitherto referred to as detector pairs) in the ring. By using proper timing information, it is possible to form a line connecting two detector pairs, known as a line-of-response (LOR). By collecting many LORs, it is possible, using mathematics explained later, to create an image displaying the annihilation intensity for each point, which directly corresponds to the desired functional data. By timing the delay in photon arrival, the LORs can be "localized" – they can be blurred to a Gaussian distribution describing the area where the photons most likely came from.

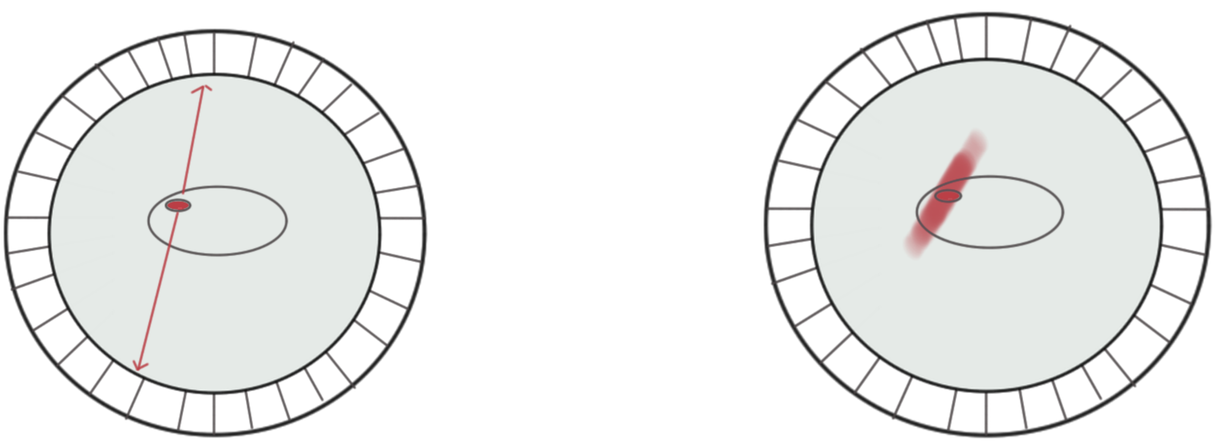

Figure 1. Left: A ring of scintillators surrounds a patient. Upon an annihilation event, two antiparallel photons will be collected by the ring. Right: A Gaussian-blurred LOR indicating the most probable area of the annihilation event.

Thus, the fundamental detection geometry in PET – as in all forms of tomography – is a ring surrounding the patient. In modern commercial PET scanners, there are often several rings of detector pairs stacked on top of each other to maximize the number of photons collected. As one would imagine, with several rings, each roughly 5 feet in diameter and each consisting of scintillators cut into 1-cm^2 pieces that are connected to photomultiplier tubes, the price can grow exponentially. While this method works, an ideal detector would consist of a geometry that maximizes photon collection efficiency and image resolution by providing a large collection range and fast timing resolution while simultaneously minimizing cost.

The strip PET detector

Recent literature has begun to explore the possibilities of using cheaper, more robust scintillators and photodetectors and new detector geometries. One such method, the focus of our research, is the strip PET, first proposed by Moskal et al. in 2013. This detector geometry relies on longitudinal strips surrounding the patient with photodetectors on either side of the strip, as depicted in the figure below.

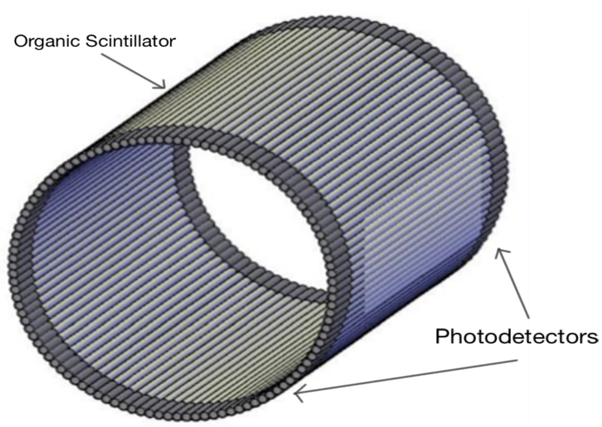

Figure 2. The Strip-PET detector. This configuration relies on longitudinal organic scintillators coupled to photodetectors on either extremity.

In contrast to relying heavily on photon stopping power using inorganic scintillators, the strip PET will rely largely on timing information, depicted in figure 3. By measuring the delay in time of arrival of the scintillator signal to either photodetector in a strip, we can locate the impact point within two opposite strips and thus form a LOR.

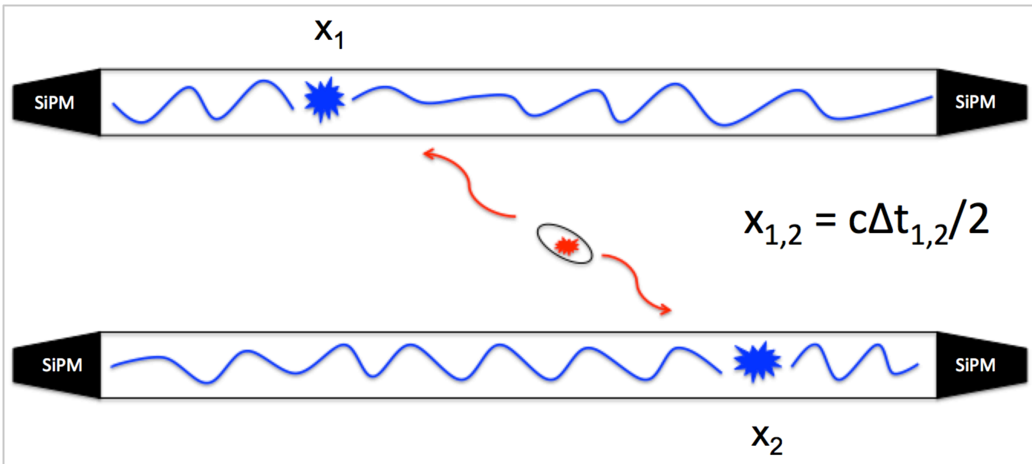

Figure 3. By timing the time delay between two photodetectors in a strip, we can calculate the point in the strip where the photon impacted. From there, we can form a LOR between two opposite strips as one would normally with standard PET. The result is a Gaussian-profiled ellipse of uncertainty for the original annihilation event.

Our strip PET design utilizes organic scintillators (bc404, Saint-Gobain Crystals) and semiconductor photodetectors –avalanche photodiodes and silicon photomultipliers. Tests are still currently being done to determine which photodetector is ideal. We have designed the equipment and created a prototype. Now we are focusing on characterizing the individual scintillators and photodetectors and characterizing their utility when combined.

CHAPTER II

BACKGROUND AND METHODS

Scintillators

A scintillator is a material with the ability to absorb ionizing radiation and to convert a fraction of the absorbed energy into visible or ultraviolet photons. The conversion process typically takes place on a time scale of nanoseconds to microseconds, producing a brief pulse of photons within the scintillator material. Photodetectors detect the light pulse whose intensity is proportional to the energy deposited in the scintillator and convert it into electrical signal.

Modern PET scanners use inorganic single-crystal scintillators because of their generally higher density and atomic number, allowing better detection efficiency. However, they are relatively slow and expensive. The amplitude distribution of the pulses collected by photomultipliers allows determination of a place where the gamma quantum reacted with accuracy equal to the size of a small crystal element. In further analysis, in order to determine a LOR, it is assumed that the gamma quantum has been absorbed in the middle of the detector element. This assumption is one of the main variables that limit resolution of the images. All current scanners use, for the detection of gamma quanta, the photoelectric effect and in the event selection the energy discrimination window, typically in the range from 350 keV to 650 keV, is applied. This reduces the noise caused by the annihilation quanta scattering in the patient's body. Such energy window corresponds to the angular range of scattering from 0 to about 60 degrees.

A way to improve the resolution of the tomographic image is determination of the annihilation point along the line-of-response based on measurements of the time difference between the arrivals of the gamma quanta to the detectors. In practice, due to the finite resolution of the time measurement, it is possible to determine only a section along LOR in which the annihilation had occurred with the probability density determined by the time resolution. This improves the reconstruction of PET images by improving signal to noise ratio due to the reduction of noise propagation along the LOR during the reconstruction.

We are using an organic plastic scintillator called Bicron BC 404 (Saint-Gobain Crystals) that has low density, short decay time constant and is much cheaper than inorganic scintillators. It has a decay time of less than 2.5 ns. Organic scintillators allow better time resolution due to low density and lighter elements in the manufacturing materials; i.e. carbon-hydrogen plastics. According to Moskal et al. (2013), "enlargement of the thickness enables efficient detection of gamma quanta using organic plastic scintillators, which are characterized by excellent time resolution, which is order of magnitude better in comparison with the fastest inorganic scintillators". The new PET scanner is made of long plastic scintillators and has lower stopping power, which means more photons can reach the photodetectors at either end of each scintillator strip. A larger longitudinal field of view would allow for simultaneous imaging of larger fraction of the body. In the case of current PET scanners such image of a whole body requires performance of many independent measurements in steps taken moving the patient inside the scanner by about half the width of the ring. Thus, in case of the whole body examination, an increase of the longitudinal field view by a given factor would increase statistics of registered events by the same amount. Organic scintillators are easy to produce various shapes and sizes while retaining the number of photomultipliers used. Because of this shaping property, scintillators plates can be used instead of inorganic crystal blocks to cover more surface area of the patient's body allowing better results.

Image formation

As discussed in previous sections, a PET detector array will find coincident photon triggers and create a line of response (LOR) that can be used to form an image. Ideally we would be able to use a more traditional reconstruction technique such as computed tomography or single-photon emission computed tomography. However, the method of data collection in PET does not allow for such techniques to be used. So, PET data are often presented in forms analogous, but not identical, to computed tomography. There exist several methods for reconstruction in PET, but most have rounding errors that are not favorable when trying to pinpoint a concentration of cancerous cells. The defining mathematical method of tomographic image formation is the Radon Transform, first theorized in the early 1900s. For an unknown function f, which, in tomography may represent the attenuation-coefficient function, is defined for each (s, θ) (Feeman 2010). The Radon Transform, which is essentially a line integral across each angular component of a two dimensional plane, may be expressed as:

$$\text{Radon Transform of } f = \boldsymbol{R}f(s, \theta) = \int_{l_{(s,\theta)}} f \, ds$$

This method of data acquisition only allows consideration of LORs in a single imaging plane. The data of all line integrals along a given angle is called a projection, and the organization of all projections is typically shown as a sinogram, seen in figure 4 (Alessio and Kinahan, 2006).

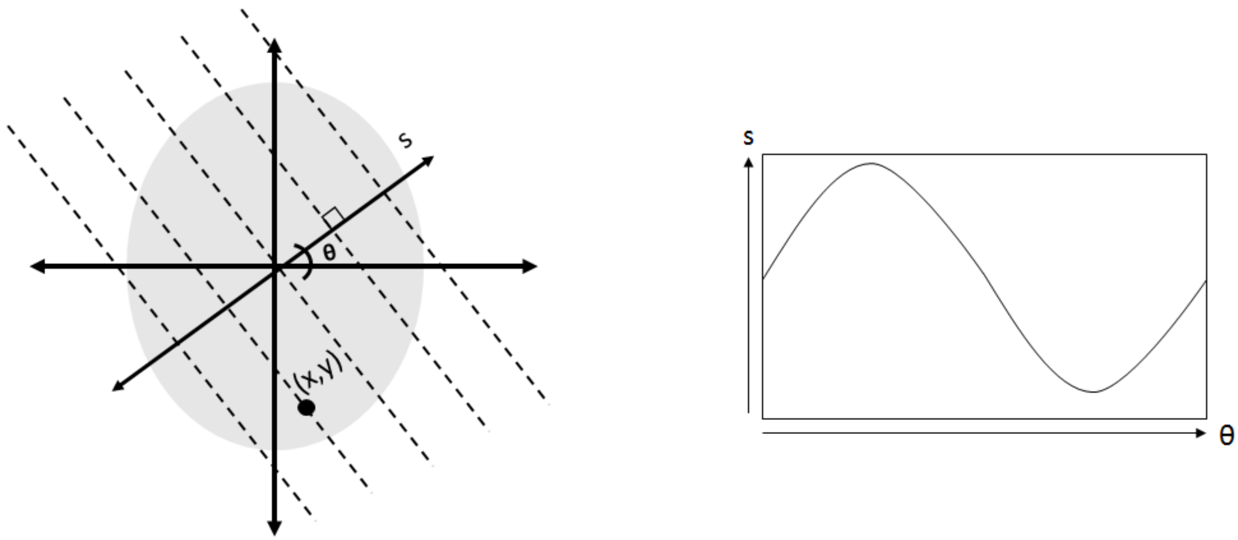

Figure 4. Left: A line projection (given by the radon transform) across an arbitrary image. Right: A sinogram formed by plotting the radon transform.

Of course, the human body is much more complex and consists of many different tissues that all have different attenuation coefficients. Figure 5 gives a more realistic representation of a brain with targets of varying attenuation coefficients, sizes, and shapes.

With this widely used method, we obtain a single two-dimensional slice of a three-dimensional body, and we can reconstruct the full three-dimensional body by stacking image slices.

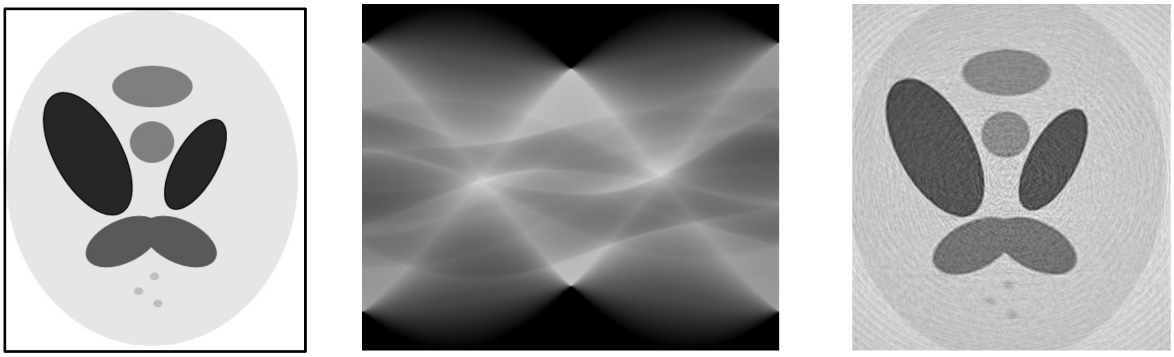

Figure 5. Left: A model cross-section of a brain with varying attenuation coefficients, shown by gray scale. A sinogram of such a brain may look like the one shown in the middle. Right: The inverse radon transform of the sinogram in the middle.

Equipment characterization

To begin testing the strip PET, we prepared two 18 cm bc404 crystals coupled to either avalanche photodiodes or silicon photomultipliers. Using timing we can calculate the hit positions within the scintillators then again extrapolate the position of the annihilation. We were able to emulate the positron-electron annihilation with radioactive isotope 22-Na. Using photomultiplier tubes we found we were also able to use energy discrimination as a parameter to calculate the hit locations.

Hardware Setup

We started with only two strips first, now we are using four strips to collect the data. We are using Sodium-22 as our source. It releases two back-to-back photons at energies of 511 keV and 1274.5 keV. The detector array consists of bc404 plastic scintillators and photomultiplier tubes for high timing resolution.

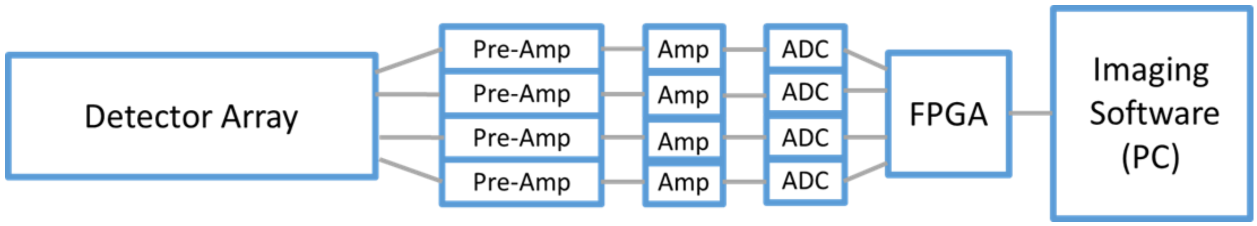

Figure 6. The detector array collects photon emitted by our radioactive sample. The electrical signal from the photodetectors is then send through pre-amplification and amplification for filtering and signal strengthening. This data is then quickly processed in an FPGA and sent to the computer, where image reconstruction is performed.

Light signals from each strip are converted to electrical signals by two photomultipliers placed at opposite edges. The detector is connected to pre-amp and amplifier which improves signal to noise ratio. High frequency ADC of 5Gsps is connected to it for high timing resolution. A field-programmable gate array (FPGA) is connected next to determine coincidence data and reduce memory load. We can either do time measurement or the energy measurement to determine the location of coincident annihilation and line of response.

Energy Measurement

From the PMT signal we can obtain the energy on each side of the scintillator. The difference over sum ratio for V_{rms} of each photodetector may be used to observe a linear trend along the scintillator, indicating that we can potentially use energy characterization to locate the hit position with the scintillator.The closer the hit to the PMT the higher the energy and further the hit lower the value of energy. We can see that if energy hits on at the center we tend to get the ratio zero.

Time Measurement

The hit position versus the center of the scintillator is determined based on time difference measured on both sides of the scintillation strip. The time at which gamma quantum hits the module can be determined as an arithmetic mean of times measured on both sides of the module. Position (x) along the line of response is determined from time difference between the photons, as depicted earlier in figure 3. The position of x with resolution of time-of-flight measurement would result in the determination of the annihilation point along the line-of-response with accuracy.

Software

MATLAB software produces sinogram and images of the data. After the sources gives off back to back photon, the coincidence point is measured using 2 APD detectors with Barium 356keV source. All data is filtered with 1V threshold and searched for 2 events that occurred within 10ns intervals of each other. The differences of a coincidence event: voltage peak heights and rise times is measured. The detector array returns the detector location and time of hit. The algorithm helps to find the hit location on each scintillator. We use time proportionality to find the source location. Then we can use the data to make histogram image. The line of response allows us to then use the radon transform to perform successful image reconstruction. We get sinogram from a radon transform and the inverse of the Radon transform can be used to reconstruct the original density from the projection data. Superposing (stacking) all of the two-dimensional images will give us a 3D image. And that is how we get the functional metabolic image of different organs.

CHAPTER III

RESULTS

The scope of this project is an incredibly large one and it is impossible to complete over just one years time. However, the initial testing of the strip scintillators gives a positive outlook for the completion of this design. It is hopeful that with further testing it will be possible to continue to improve on the design based around the strips. Currently we have built and completed characterization of a full strip outfitted with photodetectors. By using only energy profiles of the pulses, it was possible to determine the position of the origin of the pulse within a reasonable standard deviation, as demonstrated below.

Initially only three points along the strip were chosen to test, all measured as distances from the same end of the set-up. These points (3 cm, 9 cm, and 15 cm) were chosen to give a general idea as to whether the resolution would be satisfactory to continue with testing and characterization. These positions were given values based on the difference of their energy profiles divided by the sum, called the gamma value:

$$\gamma = \frac{V_{rms,left} - V_{rms,right}}{V_{rms,left} + V_{rms,right}}$$

As shown below, the data fit the line excellently, allowing for more measurements to be taken as closer intervals.

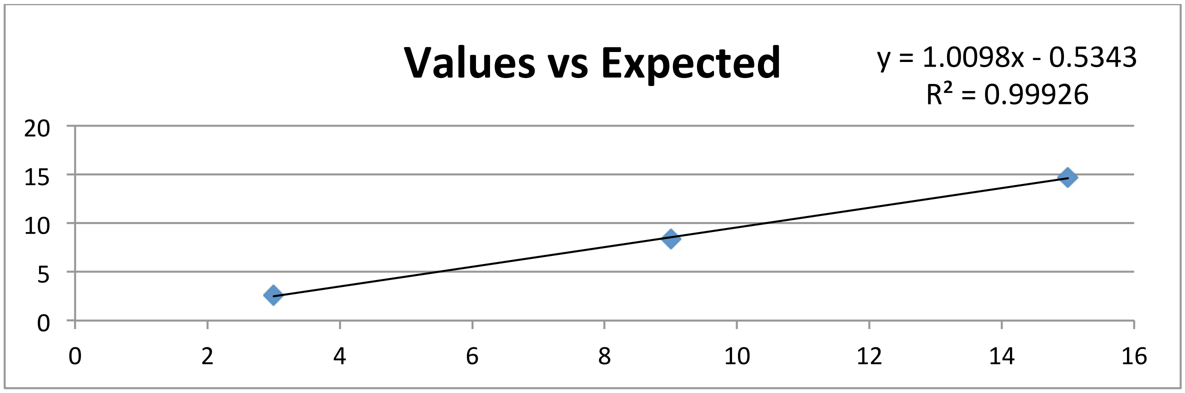

Figure 7. Scintillator characterization of Experimental Values (y-axis) vs. Expected Values (x-axis). The data shows a clear linear trend, indicating the we are able to predict the hit location within the scintillator relatively accurately.

It was also critical to characterize the resolution more closely at each of these positions. To do this, the data was taken from each point and the frequency of each deviation from the actual position was charted in the histograms shown below. Each of these measurements gave a general standard distribution centered on zero and with relatively similar standard deviation, shown in Appendix I.

The significance of these results is crucial. Again, while it is difficult to predict the final outcome of the overall project and the original design, the current data as displayed above show signs of further success in the future. This data shows that, while not exact with only one, short strip, it will be possible to increase the efficiency of this detection system. With a final length of ~2 meters, it will be possible to also use the time difference between the detections to reconstruct these positions and compare with the energy profiles. As the ring of scintillators is completed and the length of the strips is extended, the resolution should increase tremendously. The work done so far is a promising step toward the construction of a safer, more effective, more efficient scanner.

CHAPTER IV
CONCLUSIONS

Limitations

The idea to use energy discrimination was promising. Unfortunately, we were unable to effectively use this because of inconsistent instruments and short scintillator crystals resulting in near negligible discrepancies of the Gaussian energy distribution. We predict that using longer scintillator strips (our final goal is 2m each) will allow us to obtain valid energy discrimination with little blurring. Fast timing in strip PET hardware is crucial to the resolution of the image produced. Unfortunately, much of our equipment is unable to keep up with the speed of timing that we need, which further limits our progress. Regardless, this did not deter us from finding the potential in strip PET – even using solely energy characterization has given us positive-seeming results.

Future plans

While we have made some progress in the scintillator and photodetector characterization, there is still a long way to go. Our results thus far indicate that, to a certain degree of accuracy, we are able to pinpoint the hit location within a strip, opening the possibility of forming a LOR using strips. Our next steps will be to couple the energy discrimination with timing discrimination to further improve the image resolution and open up more possibilities for image formation.

If we are successful in obtaining proper timing and energy resolution, we will then move on to analysis of multi-strip PET and image formation using radioactive samples and image phantoms. Ideally, using both energy and timing, we will be able to properly characterize, to a Gaussiandistributed error, both the hit location of a photon in the strip and, as mentioned earlier, the original location of the photon to a “ellipse of uncertainty”. If two-strip and four-strip PET are successful, we will hopefully be able to get funding to build a fully-functioning PET prototype and, from there, demonstrate the full potential that we see in this newer, cheaper, and (hopefully) better PET scanner design.

REFERENCES

Moskal, P., et al. (2013). "Novel detector systems for the positron emission tomography." arXiv preprint arXiv:1305.5187.

Spanoudaki, V. C. and C. S. Levin (2010). "Photo-detectors for time of flight positron emission tomography (ToF-PET)." Sensors **10**(11): 10484-10505.

van Beek, E. J. and E. A. Hoffman (2008). "Functional imaging: CT and MRI." Clinics in chest medicine **29**(1): 195-216.

Logothetis, N. K. (2008). "What we can do and what we cannot do with fMRI." Nature **453**(7197): 869-878.

Ollinger, J. M. and J. A. Fessler (1997). "Positron-emission tomography."

Fahey, F. H. (2002). "Data acquisition in PET imaging." Journal of nuclear medicine technology **30**(2): 39-49.

Alessio, A. and P. Kinahan (2006). "PET image reconstruction." Nuclear Medicine **2**.

Feeman, T. G. (2010). The Mathematics of Medical Imaging, Springer.

APPENDIX

IMPORTANT PLOTS

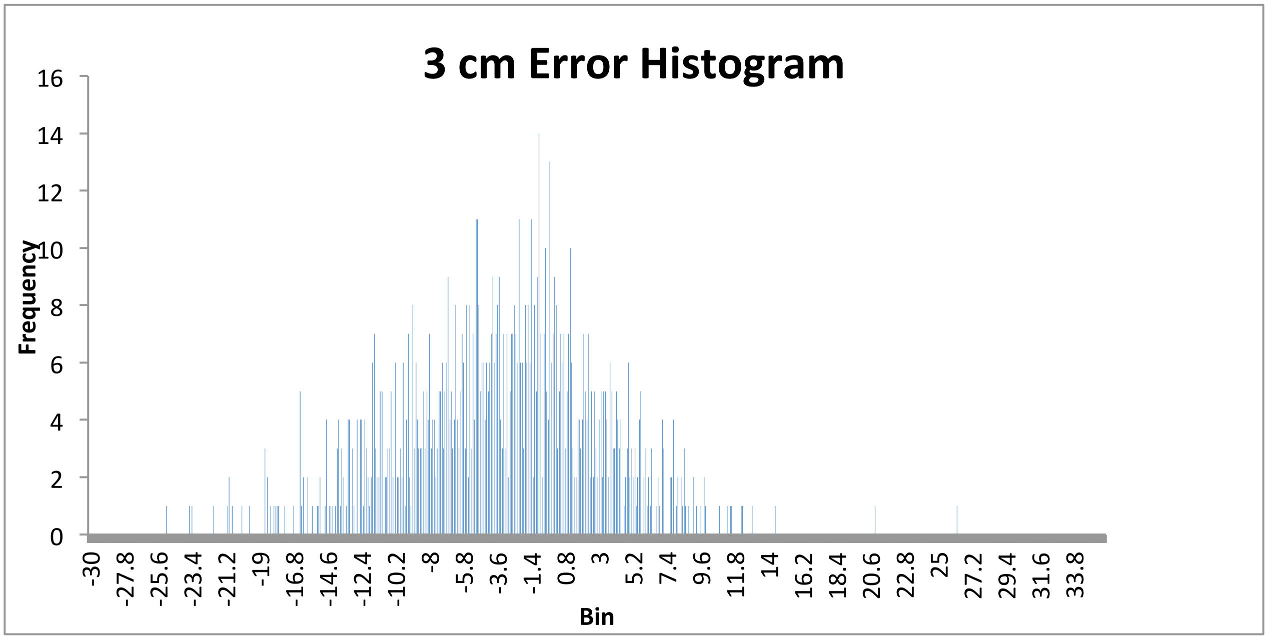

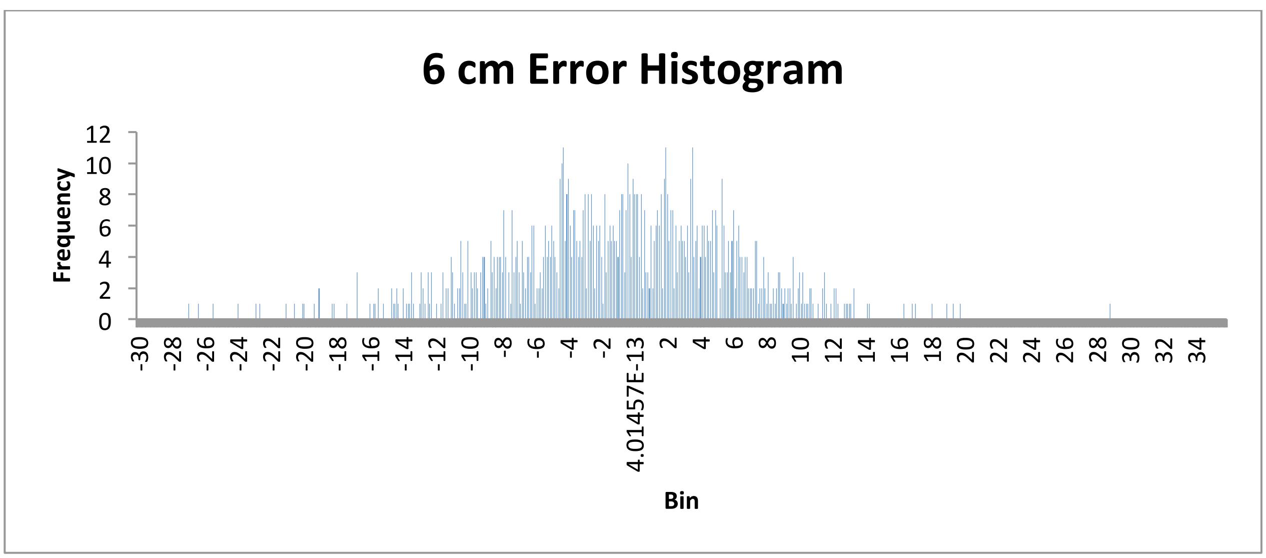

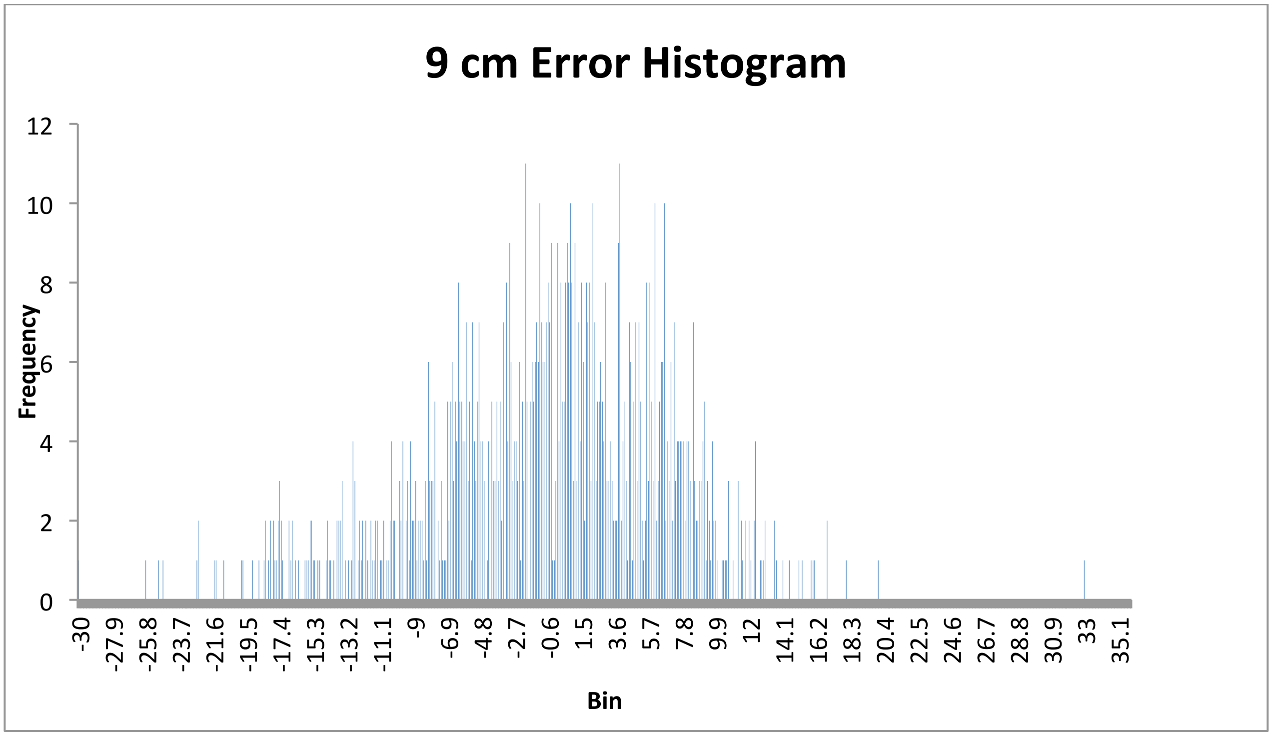
9 cm Error Histogram
Frequency
Bin
12
10
8
6
4
2
0
-30
-27.9
-25.8
-23.7
-21.6
-19.5
-17.4
-15.3
-13.2
-11.1
-9
-6.9
-4.8
-2.7
-0.6
1.5
3.6
5.7
7.8
9.9
12
14.1
16.2
18.3
20.4
22.5
24.6
26.7
28.8
30.9
33
35.1

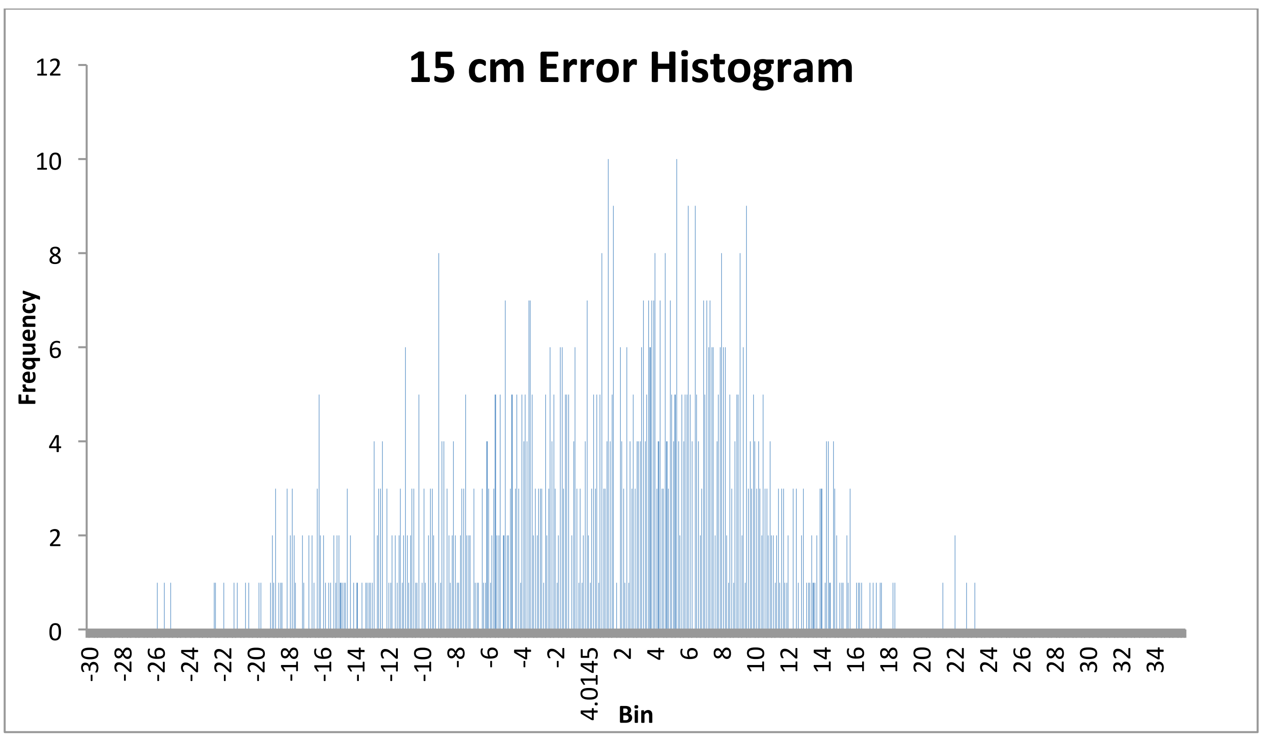
15 cm Error Histogram
Frequency
Bin
12
10
8
6
4
2
0
-30
-28
-26
-24
-22
-20
-18
-16
-14
-12
-10
-8
-6
-4
-2
4.0145
2
4
6
8
10
12
14
16
18
20
22
24
26
28
30
32
34